International Journal of Fracture **63**: 155–171, 1993.

Weld magnification factors for semi-elliptical surface cracks in fillet welded *T*-butt joint models

B. FU,[1] J.V. HASWELL[2] and P. BETTESS[1]
[1]*Department of Marine Technology, University of Newcastle upon Tyne, Newcastle upon Tyne NE1 7RU, UK*
[2]*British Gas plc, Engineering Research Station, Newcastle upon Tyne NE99 1LH, UK*

Received 26 February 1993; accepted in revised form 23 July 1993

Abstract. The weld magnification factor method has been widely used in the determination of the stress intensity factor (SIF) for weld-toe cracks in welded structural components. Weld magnification factors M_k are normally derived from two-dimensional crack models with fillet weld profiles to take account of the effect of weld-notch stress concentration at the deepest point of the crack front. This paper presents a detailed three-dimensional analysis of weld-toe surface cracks in fillet welded T-butt joint models using the finite element method. Effects of the weld notch and the welded attachment stiffness on the SIFs of the weld-toe surface cracks have been studied quantitatively. Weld magnification factors applying to the whole surface crack fronts have been estimated. Numerical results show two contradictory effects; that the effect of weld notch increases SIF values throughout the shallow surface crack fronts which are in the region of notch stress concentration, while the effect of local structural constraint reduces the SIF values. The increase in the SIF values mainly depends upon the relative crack front depth and the decrease in the SIF values mainly depends upon the crack shape aspect ratio for a specific weld profile. Both effects on the weld magnification factors can be estimated separately. A simple approach for deriving the weld magnification factors for various weld-toe surface crack problems is proposed for engineering applications.

1. Introduction

Surface cracks often occur in the welded joints of many engineering structures. The practical analysis of such cracks is of major importance in fatigue and fracture assessments. The joints have complex local geometries which result in a complex stress system at the weld toe, including a localised notch region with high stress gradients. This effect increases the stress intensity factor (SIF) value. The welded attachment contributes an additional local constraint, which tends to reduce the SIF value. Both effects apply to the whole front of the weld-toe surface cracks.

Although such surface cracks are practical engineering defects, the three-dimensional (3D) geometries are difficult to model. This has restricted comprehensive analysis to simple surface cracks in either flat plate models or plain cylinder models. The weld notch effect has previously been analysed using two-dimensional (2D) edge crack models with fillet weld profiles. This approach gives a conservative estimation for the stress and SIF at the deepest point of the surfrace crack front. It meets the requirement of conventional fatigue prediction methods, by which predictions of the fatigue crack growth are based on the SIF value at the deepest point of the crack front only. However, some experimental observations of fatigue surface crack growth at welded intersections indicate that the advance of the crack front at the surface weld notch region may be faster than that through the plate thickness. This implies that the notch stress concentration has a significant effect on the shallow section of the surface crack front. Therefore, 3D modelling of surface cracks is necessary to give realistic SIF predictions for integrity assessments.

A detailed 3D linear elastic fracture mechanics analysis of relatively shallow surface cracks in a welded joint model has been carried out using the finite element (FE) method. The present study leads to an advanced understanding of the weld-notch effect on surface cracks and provides improved results for engineering applications.

2. Weld magnification factor method

Maddox [1] suggested a well magnification factor representing the weld-notch effect on SIF values of weld-toe cracks. The magnification factor M_k was defined as

$$M_k = \frac{K_I^t}{K_I^p}, \tag{1}$$

in which K_I is the mode-I SIF and the superscripts t and p refer to the welded T joint model and the plain plate model respectively. The cracked joints have usually been modelled by an edge-cracked plate with a transverse non-load-carrying fillet weld. The magnification factor quantifies an increase in the SIF value due to the weld notch stress concentration [1, 2].

The weld notch effect has been extensively investigated. Many quantitative studies have been based on the edge crack models and most published data used in engineering applications refers to the 2D analyses, such as those by Maddox [1], Smith and Hurworth [3], Niu and Glinka [4] and Thurbeck and Burdekin [5]. Limited 3D data has been published by Straalen et al. [6], Dijkstra et al. [7], Bell [8] and Fu et al. [9]. Methodologies for the assessment of surface defects in welded joints, such as those proposed in the British Standard Published Document PD 6493 [2], are usually based on the superposition of simple plate and cylinder crack SIF solutions and weld magnification factors. These methodologies assume that the weld notch effect, determined from the 2D analysis of an edge crack model, can be applied as a simple multiple to the 3D crack front SIF distributions, such as those published by Newman and Raju [10].

The 2D data is relevant to the deepest point on the crack front only. In an edge crack model, the weld notch affects the crack tip stress intensity and the effect reduces as the crack length increases through the thickness. This results in the following M_k equation [2]:

$$M_{k(a)} = C\left(\frac{a}{T}\right)^{\beta}, \quad (1.0 \leqslant M_k \leqslant K_c), \tag{2}$$

in which a and T refer to the crack depth and the thickness of the cracked plate respectively, the coefficient C and the exponent β are geometric constants depending on the weld details, such as weld angle, weld-toe radius and ratio of the attachment thickness to the plate thickness etc., the subscript (a) denotes the deepest point of the surface crack front, and K_c is the stress concentration factor for the specific weld geometry. The limiting value of K_c is justified, since the nominal value of an equivalent stress applied to the edge crack face converges to the stress concentration factor as the crack depth decreases. Similarly, the M_k factor that applies to the free surface point of the crack front has been suggested to be equal to the K_c value, because the depth of a surface crack front reduces to zero [2]. The effect of the surface crack shape has been ignored. The 2D studies have shown that the weld effect which increases the SIF values reduces

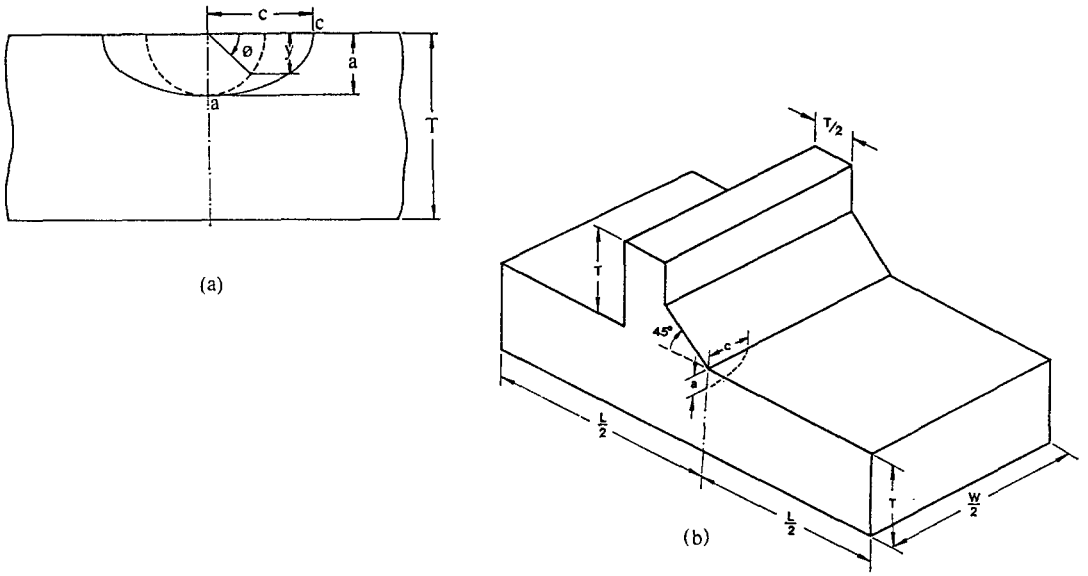

Fig. 1. Geometries of (a) the semi-elliptical surface crack in a finite plate and (b) the fillet welded T-butt joint with a weld-toe surface crack.

to zero as the crack depth increases to about 20–30 percent of the plate thickness [2]. It implies that the weld correction only applies to the 'shallow cracks', which are in the local region of weld notch stress concentration.

SIF results from limited 3D FE analyses indicate that the weld magnification effect at the free-surface position is dependent of the crack aspect ratio [6–9]. Higher aspect ratios, such as $a/c = 1.0$, imply a relatively short crack length along the weld intersection coupled with a higher structural constraint from the remaining part of the intersection. Pang [11] suggested an empirical M_k function for the free-surface crack tip as below

$$M_{k(c)} = M_{k(a)} + 1.15^{-9.74(a/T)}, \quad \left(\text{for } \frac{a}{T} \leqslant 0.15\right), \tag{3}$$

where the subscript (c) refers to the weld-toe crack tip. However, this equation remains as a function of maximum crack depth only. Based on 3D FE results and an engineering approximation, Fu et al. [9] suggested a formula for the M_k factor equation

$$M_k\left(\frac{a}{c}, \frac{a}{T}, \phi\right) = f_1\left(\frac{a}{c}\right) + f_2\left(\frac{a}{T}, \phi\right), \tag{4}$$

where ϕ is crack front parametric angle, as defined in Fig. 1a.

3. Finite element modelling of surface cracks

Detailed 3D linear elastic FE analyses of semi-elliptical surface cracks in a plain plate model and a fillet welded T-butt joint model have been carried out. The joint model, as shown in Fig. 1b, is

subjected to uniaxial tension and pure bending loads. This model represents a simplified global but detailed local weld geometry of cracked joints in engineering structures. A 45° weld angle with a sharp notch at the weld toe has been considered in the present study. The 45° angle represents an average value for those considered in most 2D studies; which show the effect of the weld angle on the M_k factor value is not significant [4]. The sharp notch-root represents the most severe weld-toe geometry. Other information on the geometric variables of the welded joint model is given in Fig. 1b. This joint model introduces a notch stress concentration and the load-free attachment provides a non-symmetric local stiffness on one side of the surface crack.

Cracks with aspect ratios $a/c = 0.2$, 0.4 and 1.0, with maximum depth/plate thickness ratios $a/T = 0.5$, 0.10, 0.15, 0.20 and 0.40 have been analysed. In addition, edge cracks in the welded T-butt plates have also been considered to provide results for the limiting crack aspect ratio $a/c = 0$. These crack models represent extreme and intermediate surface crack shapes. In order to determine the M_k factors, surface cracks in plain plates have also been analysed. The FE models of the cracked plain plates were obtained by removing the FE mesh of the welded attachment from the FE models of the cracked joints. The plate width (W) was selected to be at least 5 times the surface crack length ($2c$) in all models. These dimensions are based on studies by Newman and Raju [12], which demonstrate that for $W/2c \geqslant 5$, the SIF solution for a semi-elliptical crack in finite width plate is approximately unaffected.

FE meshes constructed using 20-node hexahedral and 15-node pentahedral isoparametric 3D solid elements for the surface crack models and 8-node quadrilateral 2D plane strain elements for the edge crack model were generated. Semi-elliptical cracks were modelled by mapping semi-circular crack front meshes onto a semi-ellipse. The crack tip was modelled using a focused mesh of collapsed elements, with $\frac{1}{4}$ point node shifting to generate the $r^{-1/2}$ singularity, as proposed by Barsoum [13]. Following the preliminary 3D FE modelling of the surface cracks [9], refined element meshes were considered, which consist of approximately 8,800 nodes of nearly 2,000 3D solid elements. A typical 3D FE mesh used in the analyses is shown in Fig. 2.

Stress analysis was carried out using ABAQUS FE computer software [14]. SIF values were determined by converting the energy release rate results, obtained using the virtual crack extension (VCE) method [15], assuming the following relationship

$$K_I^2 = \begin{cases} EG & \text{(for the free surface point in plate models),} \\ EG(1-\nu^2)^{-1} & \text{(otherwise),} \end{cases} \tag{5}$$

where E and ν are Young's modulus and Poisson's ratio of the material, and G is the strain energy release rate. In the present study, $E = 206.8$ GPa and $\nu = 0.3$.

SIF results obtained from the FE analyses are presented in non-dimensional form as

$$\tilde{K}_{Ii}\left(\frac{a}{c}, \frac{a}{T}, \phi\right) = K_{Ii}\left(\frac{a}{c}, \frac{a}{T}, \phi\right)\left[\sigma_i \frac{\sqrt{\pi a}}{\Phi}\right]^{-1}, \quad (i = t, b), \tag{6}$$

in which the subscripts t and b refer to tension and bending conditions respectively, σ_t and σ_b are the tension stress and the maximum bending stress, and Φ is the complete elliptic integral of the second kind, defined by

$$\Phi\left(\frac{a}{c}\right) = \int_0^{\pi/2} \left\{\cos^2\theta + \left(\frac{a}{c}\right)^2 \sin^2\theta\right\}^{1/2} \mathrm{d}\theta, \quad \left(0 < \frac{a}{c} \leqslant 1\right). \tag{7}$$

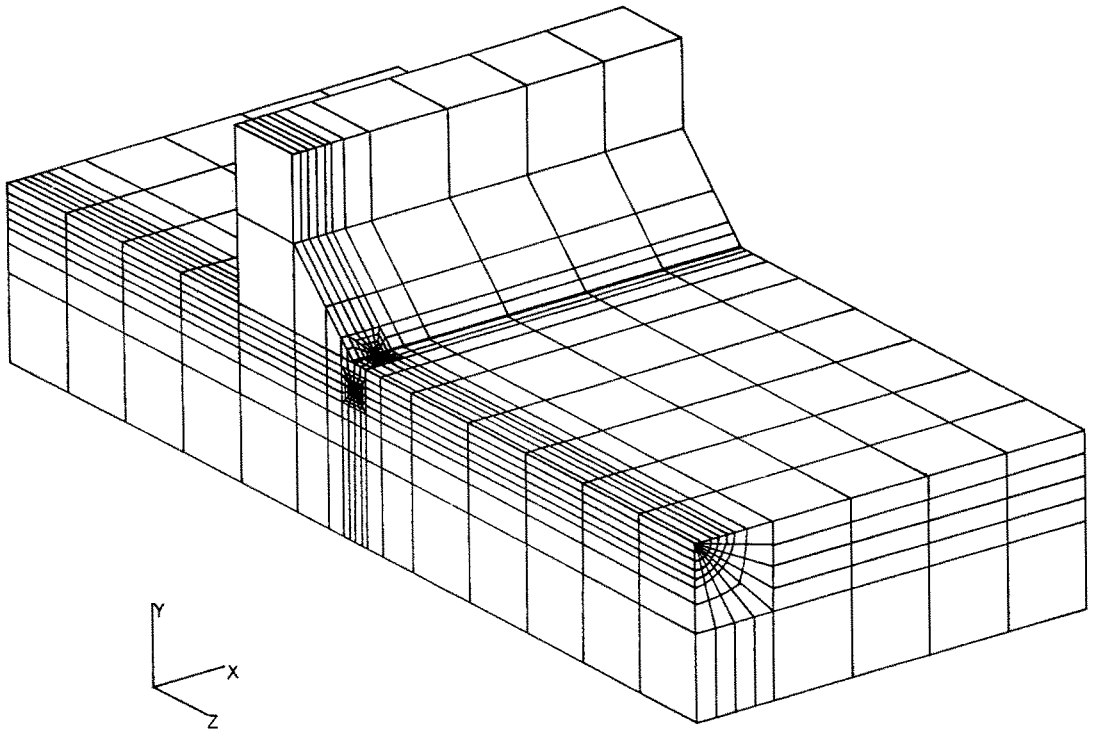

Fig. 2. Typical 3D finite element mesh for the semi-circular weld-toe surface crack model.

For the edge crack models, the normalised SIF is defined by

$$\tilde{K}_{Ii}\left(\frac{a}{T}\right) = K_{Ii}\left(\frac{a}{T}\right)\{\sigma_i\sqrt{\pi a}\}^{-1}, \quad (i = t, b). \tag{8}$$

Mode-II and mode-III singularities exist due to the lack of symmetry on the crack plane in the T-butt joint models, and the intensities of the mode-II and the mode-III singularity are dependent on the crack front depth. The G values estimated may include these intensities. However, the crack models considered in the present study are dominated by mode-I singularity, and the VCE calculation is relevant to a mode-I crack increment. Therefore, the SIF results determined using (5) are regarded as mode-I SIF values. The effectiveness of this approximation is assessed using 2D and 3D crack models in the following sections.

4. Stress intensity factor results

4.1. SIF results for the edge crack models

Edge cracked T-butt joint models with a crack depth a/T ranging from 0.01 to 0.40, have been analysed. This models an extended crack shape, $a/c \to 0$, which represents the limit of the ratio a/c as $c \gg a$. In this case, the SIF at the deepest point of the crack front is unaffected by the crack shape.

Mode-I and mode-II SIF values were determined using the relationship between the SIF and the relevant crack face opening displacements (CFOD) near the crack tips. Numerical results of the CFOD values were corrected using a compensation method [16], and the mode-I SIF results were compared with the SIF values approximated from the VCE results.

The results, shown in Fig. 3, demonstrate that both K_{I} and K_{II} values for the welded joint model increase rapidly as the crack depth reduces. The SIF values for the joint model converge to the SIF values for the plate model as the crack depth a/T reaches approximately 0.30. This shows the significance of the weld-notch effect as the crack front depth is withn the region of local stress concentration. Mode-II SIF values obtained are much lower than the mode-I SIF values. The mode-I SIF results determined using the CFOD method and the VCE method are almost identical. Therefore, effect of the mode-II SIF in the interpretation of the VCE results into mode-I SIF values can be ignored.

4.2. SIF results for the surface crack models

Semi-elliptical crack shapes are generally assumed in engineering models of fatigue surface cracks. The semi-circular crack, $a/c = 1.0$, represents the opposite limit to the edge crack in the study of surface cracks while the semi-elliptical crack shapes $a/c = 0.2$ and 0.4 are regarded as intermediate models. In the 3D analysis, the SIF values have been determined from the VCE results. SIF distributions for the cracks in welded T-butt joint and plain plates were predicted using identical FE meshes for the cracked plates.

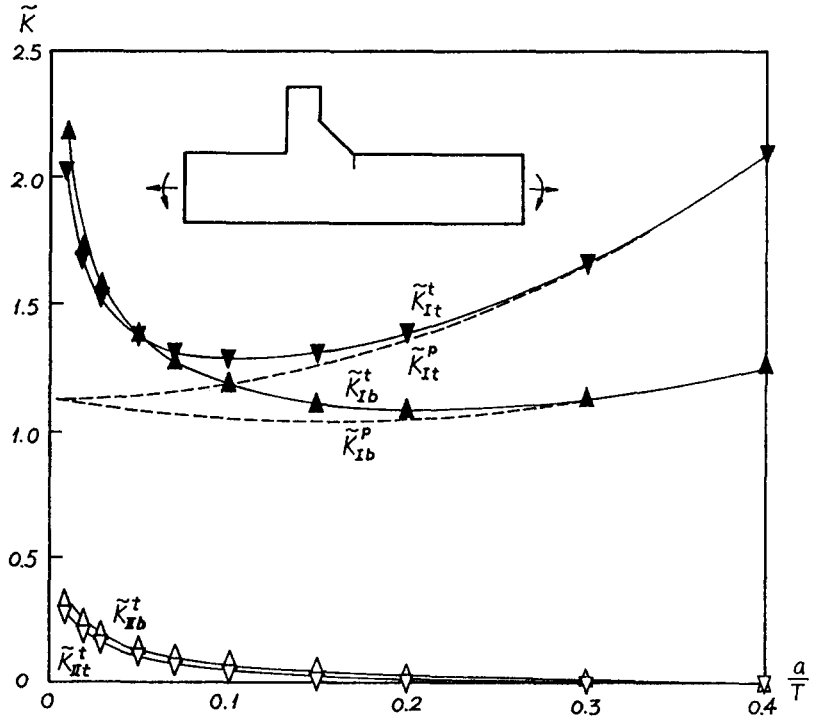

Fig. 3. Normalised SIF values for the edge cracks in the welded T-butt joints (the superscripts t and p refer to the T-butt joint and the plain plate models, respectively, and the subscripts t and b refer to tension and bending loads, respectively).

The SIF results for surface cracks in plain plate models were compared with Raju and Newman's FE results [17]. Good agreement was obtained for the SIF results subjected to tension load, while up to 15 percent of difference between the present FE results and Newman and Raju's empirical SIF equation [10] were obtained for bending load. The maximum difference occurs at the free-surface crack tip. It has been claimed that up to 5 percent of difference is generally included in the SIF equation and the SIF value predicted for the crack tip at free surface intersection will be even higher than FE results [12]. The difference is also dependent upon the methods used to derive the SIF value, particularly at the free surface. However, the difference does not significantly affect the estimation of the M_k factors, because the K_I^i and the K_I^p values are related to the same crack tip element mesh and are derived using the same method.

SIF distribution obtained for the surface cracks in the welded T-butt plates confirm the effect of the weld-toe notch discussed for edge cracks. Figure 4 shows comparisons of the SIF values at the deepest point of the surface crack front in the T-butt joints and the plain plates against the maximum crack depth a/T. It demonstrates that the SIF values for semi-elliptical surface cracks are bounded by the SIF values for 2D edge cracks and semi-circular surface cracks. The SIF values increase rapidly for the shallow cracks in the T-butt joints, as is also shown by the 2D analysis. However, the 3D results indicate that the SIF for the T-butt joint model does not converge to that for the plain plate model as the crack depth increases, but remains below it.

Figure 5 shows comparisons of the SIF distributions for the semi-elliptical surface cracks $a/c = 0.2$. It demonstrates that the SIF values increase significantly in the crack front section close to the notch root, and otherwise reduce to below the SIF distributions for the plain plate.

As a sharp notch at the weld-toe has been modelled in the FE analysis, a notch singularity is introduced along the remaining uncracked intersection. This increases the singularity order of the weld-toe crack tip and disturbs the crack-tip stress field around the weld intersection. Consequently, the VCE calculation for the weld-toe crack tip is contour-dependent. The effect is

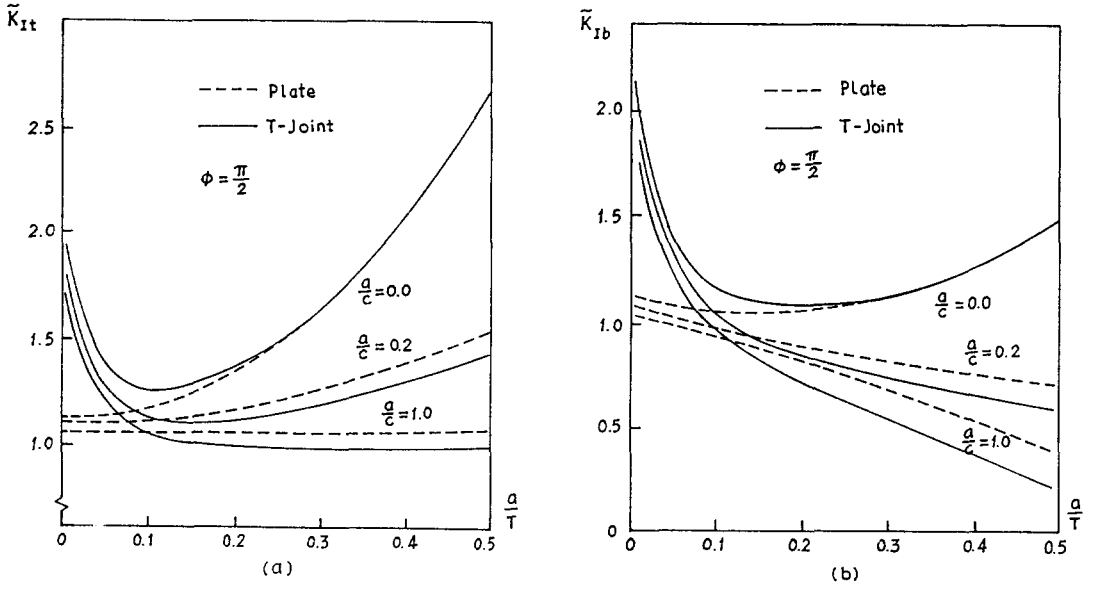

Fig. 4. Comparison of normalised SIF values for the deepest point of the surface crack front in the welded T-butt joints and the plain plates subjected to (a) tension and (b) bending.

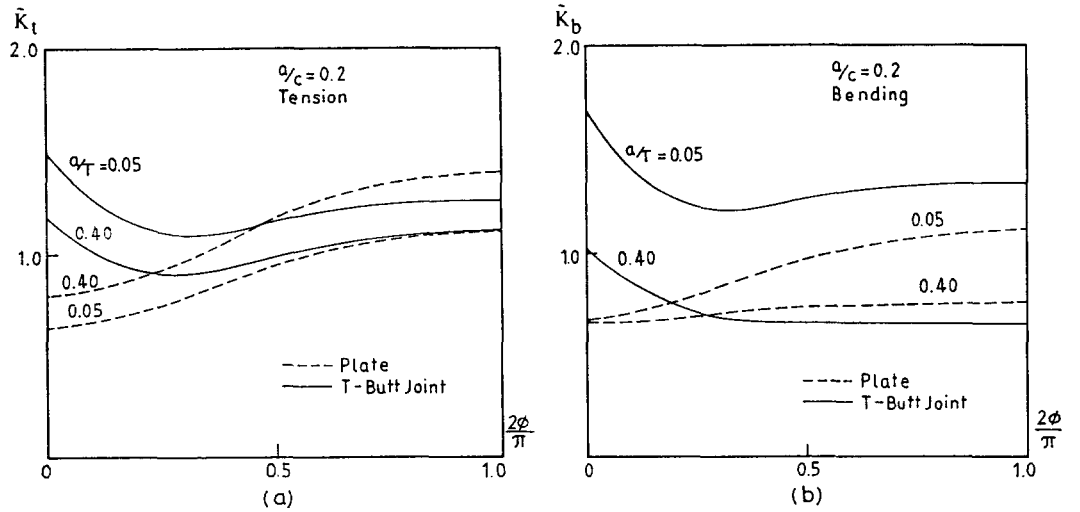

Fig. 5. Comparison of normalised SIF distributions for surface crack front in the welded T-butt joints and the plain plates ($a/c = 0.2$, $a/T = 0.05$ and 0.40).

limited to the crack tip close to the weld intersection. Consequently, the SIF values obtained at the corner and mid-side nodes nearest the surface were not included in the derivation of the M_k factors. A study of the variation in the singularity order for these surface cracks has been carried out [16] and details of this study will be published separately. The FE results, excluding surface values, are summarized as follows:

(1) The SIF increases along all sections of the crack front located within the region of the notch stress concentration. This includes the whole crack front of the shallow surface cracks and shallow sections of the crack front of deeper surface cracks. The increase in SIF decreases to zero as the depth of the crack front increases.
(2) SIF values for the deepest points of the surface crack fronts are lower than the SIF values for edge cracks with equivalent depths. This effect reduces as the crack length increases, and is zero for the cracks of infinite length.

The 3D FE results imply two contradictory effects on the SIF distributions. The presence of the welded attachment introduces a notch stress concentration and contributes additional stiffness to the local constraint. The effect of stress concentration tends to increase SIF values depending upon the crack front depth and the effect of local constraint tends to reduce the SIF values of finite length cracks depending upon the crack shape aspect ratio. Both effects apply to the whole surface crack front.

The effect of mode-II and mode-III singularities is assessed by comparing the distributions of opening, sliding and tearing displacements, obtained from the near-tip locations along the surface crack front. Normalised displacement values are compared in Fig. 6. It is shown that

(1) the sliding and tearing mode displacements are much smaller than the opening mode displacement and
(2) distributions of the opening mode displacements for plain plate and welded T-butt joint models are consistent with SIF distributions predicted using the VCE method.

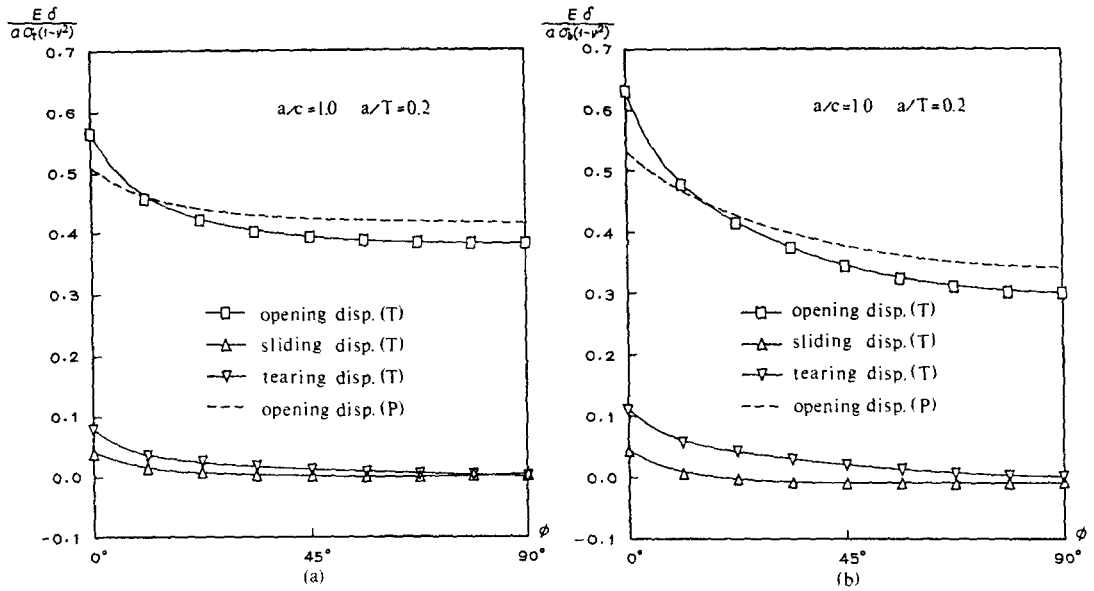

Fig. 6. Comparison of normalised near tip crack face displacements for surface crack ($a/c = 1.0$, $a/T = 0.2$) in the welded T-butt joint (T) and the plain plate (P) subjected to (a) tension and (b) bending.

This indicates that the effect of mode-II and mode-III singularities on determination of the mode-I SIF in the present study can be ignored and the mode-I SIF distributions predicted can be considered as representative and realistic.

5. Weld magnification factors for the weld-toe cracks

5.1. M_k factors for the edge crack models

M_k factors as a function of the crack depth a/T were determined, as plotted in Fig. 7. A fitted M_k equation, which applies to the whole range of crack depths affected by the notch stress concentration, has been derived using the statistical software, RS/1[18]. The fitted equation was based on the smallest residual sum of squares giving the best regression to the function assumed. The equations derived for the edge crack models subjected to tension and bending are

$$M_{kt}\left(\frac{a}{T}\right) = 0.9755 + 1.7261\left(1.0 + 76.9069\,\frac{a}{T}\right)^{-1.2879}, \tag{9}$$

$$M_{kb}\left(\frac{a}{T}\right) = 0.9249 + 2.9014\left(1.0 + 266.4478\,\frac{a}{T}\right)^{-0.7916}. \tag{10}$$

Standard deviations for the above regressions are 0.0126 and 0.0112 respectively. The M_k values predicted using the above equations are compared with the FE results, as shown in Fig. 7.

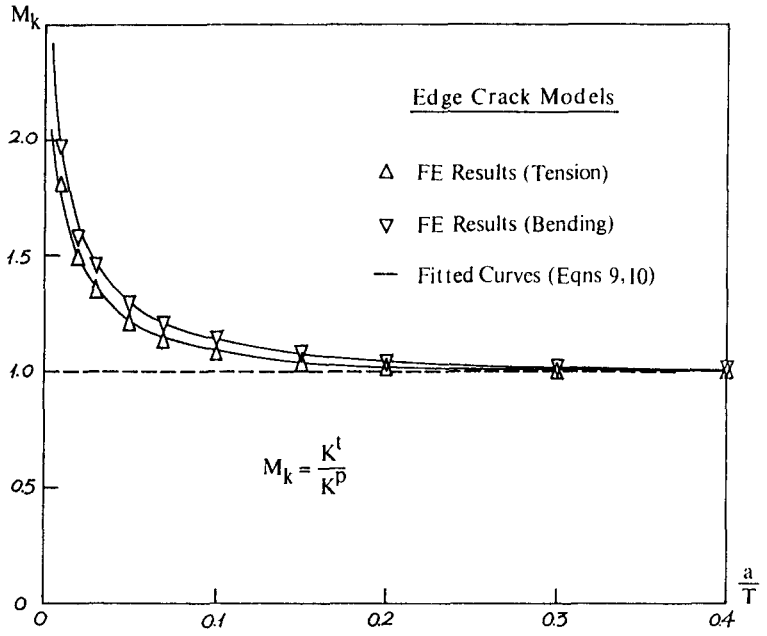

Fig. 7. Comparison of the M_k factors for the edge crack model, determined using FE results and predicted using the fitted functions.

5.2. M_k factors for the surface crack models

The weld effect on surface cracks has been quantified by comparing the M_k values obtained for different crack fronts with the same relative depth, i.e. the M_k results for the surface cracks are represented as a function of relative crack front depth y/T which is defined by

$$\frac{y}{T} = \frac{a}{T}\sin\phi, \quad (0^\circ \leqslant \phi \leqslant 90^\circ) \tag{11}$$

as shown in Fig. 1a. The M_k values are plotted against the crack front depth y/T for the surface crack shapes $a/c = 0.2$ and 1.0 in Figs. 8 and 9 respectively. These show that variations of the M_k factors for the surface cracks are similar to those for the edge crack models. Excluding the FE results for the corner and mid-side nodes nearest the surface which are subject to modelling errors, the plots of M_k factors for the surface cracks show a common dependence on the relative crack tip depth for a given crack aspect ratio. The plots imply that the effect of notch stress concentration reflected in the M_k factors for cracks of a given aspect ratio can be approximated as a function depending on the crack front depth y/T only. M_k values plotted for the deepest points against the surface crack shape aspect ratio (a/c) in Fig. 10 imply that the effect of the local constraint on finite length surface cracks can be estimated separately.

5.3. Weld magnification fractor equation

Based on the engineering judgement, it was assumed that the values of the M_k factors increases along the crack front to a maximum at the surface, and that the maximum M_k for a specific

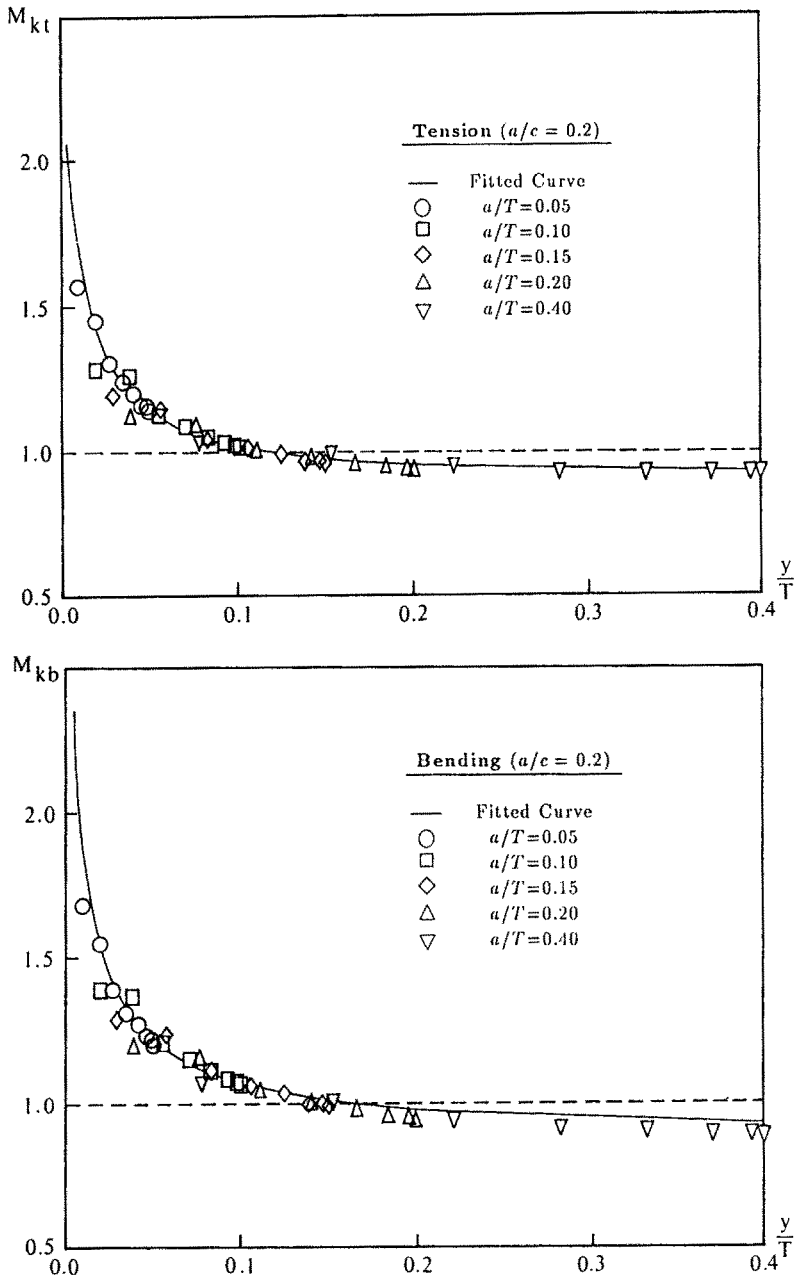

Fig. 8. Comparison of the M_k factors for semi-elliptical surface cracks ($a/c = 0.2$, $a/T = 0.05$–0.40) determined using FE results and predicted using the fitted functions.

crack depth decreases as the aspect ratio increases. M_k factor equations based on (4) were derived by curve fitting results obtained for the range of crack aspect ratios $0.0 \leqslant a/c \leqslant 1.0$, and crack depth $0.0 < a/T \leqslant 0.4$, as

$$f_1(1.0) \leqslant f_1\left(\frac{a}{c}\right) \leqslant f_1(0.0) = 1.0, \tag{12}$$

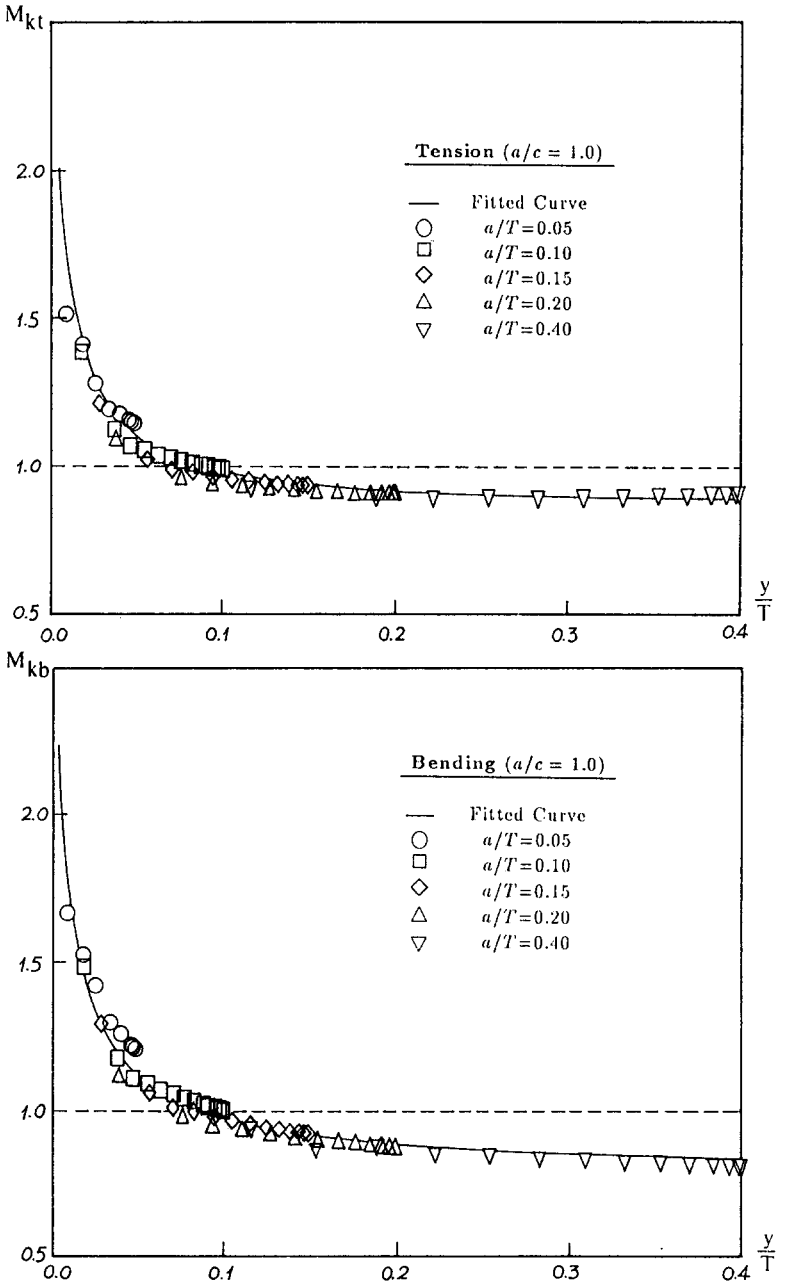

Fig. 9. Comparison of the M_k factors for semi-circular surface cracks (a/c = 1.0, a/T = 0.05–0.40) determined using FE results and predicted using the fitted functions.

and

$$f_{2t}\left(\frac{a}{T}, \phi\right) = -0.0245 + 1.7261\left(1.0 + 76.9069\,\frac{a}{T}\sin\phi\right)^{-1.2879}, \tag{13}$$

$$f_{2b}\left(\frac{a}{T}, \phi\right) = -0.0751 + 2.9014\left(1.0 + 266.4478\,\frac{a}{T}\sin\phi\right)^{-0.7916}, \tag{14}$$

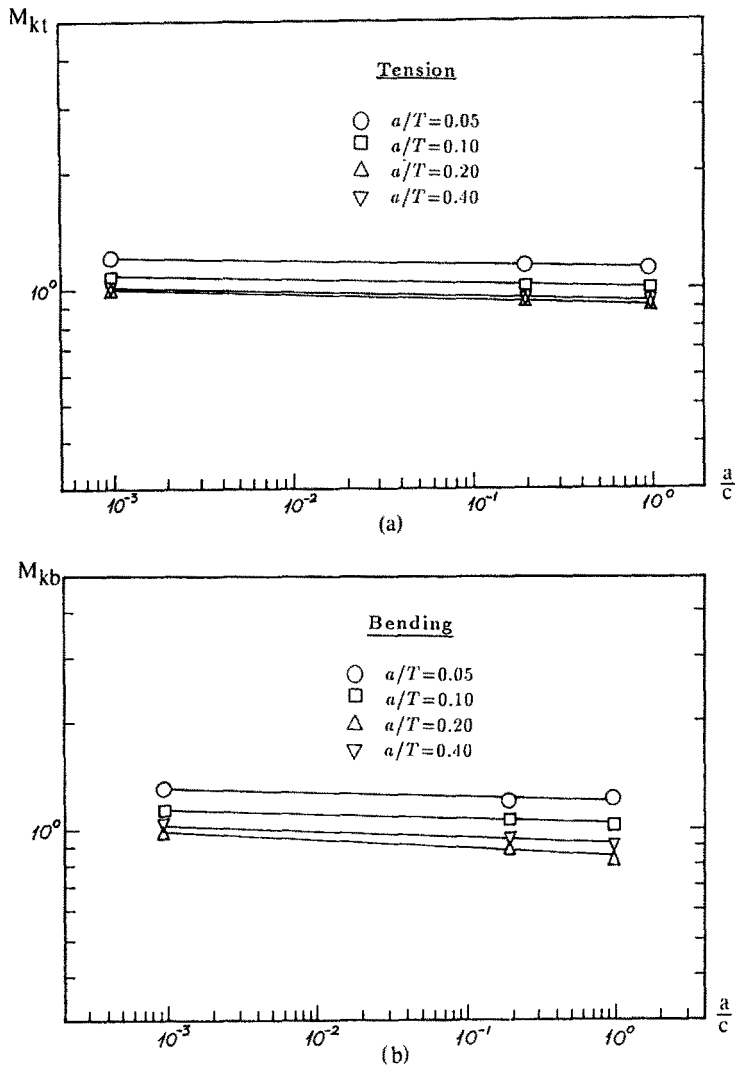

Fig. 10. Weld magnification factors for the deepest point of the surface crack fronts.

for the weld geometry considered. The value of the function $f_1(a/c)$ for intermediate crack shapes can be estimated by interpolation of the data given in Table 1.

The $M_k(a/c, a/T, \phi)$ values predicted using the above functions for the surface crack shapes, $a/c = 0.2$ and 1.0, are compared with the 3D FE results in Figs. 8 and 9. Curves for the $f_1(a/c)$ function are plotted in Fig. 11.

Table 1. $f_1(a/c)$ values for the weld magnification factor equation

	$f_1(a/c)$	
a/c	Tension	Bending
0.00	1.0000	1.0000
0.20	0.9219	0.9108
1.00	0.8860	0.8395

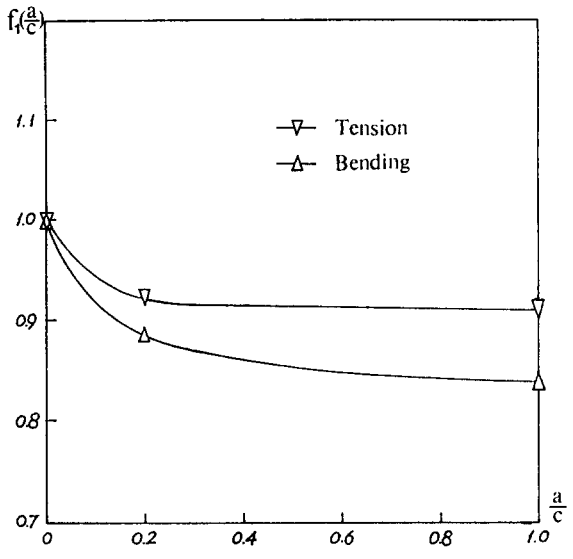

Fig. 11. The function $f_1(a/c)$ vs. the surface crack aspect ratio (a/c).

The $f_2(a/T, \phi)$ functions have been derived using the M_k equations, (9) and (10), for the edge crack models. Excluding the FE results at the corner and mid-side nodes nearest the surface, the data points shown in Figs. 8 and 9 lead to a conservative M_k approximation for crack front in local region close to the notch. Statistical curve fitting data is given in Table 2.

The above approach can be extensively applied to various joint models. An advantage of this approach is that the f_2 function can be determined from detailed 2D studies taking specific weld geometries into account while the f_1 function can be derived from limited 3D crack modelling for various crack shapes. This improves the existing 2D approach while reducing the difficulty of carrying out a large number of detailed 3D analyses for each particular problem considered.

5.4. *Modified stress intensity factor distributions for the surface cracks*

SIF distributions for surface cracks with a common aspect ratio $a/c = 0.2$ in the welded T-butt joint and in the plain plate are compared in Fig. 12. The SIF values for the plain plate models were determined using Newman and Raju's SIF equations [10] while the SIF values for the

Table 2. Deviations of the function fitting regressions for (13) and (14)

Crack shape	Loading condition	Standard deviation	Max upper deviation	Max lower deviation
0.0	tension	0.0043	0.35%	0.46%
	bending	0.0112	1.17%	1.39%
0.2	tension	0.0457	11.92%	4.94%
	bending	0.0524	12.91%	7.18%
1.0	tension	0.0426	19.23%	5.81%
	bending	0.0507	16.18%	9.92%

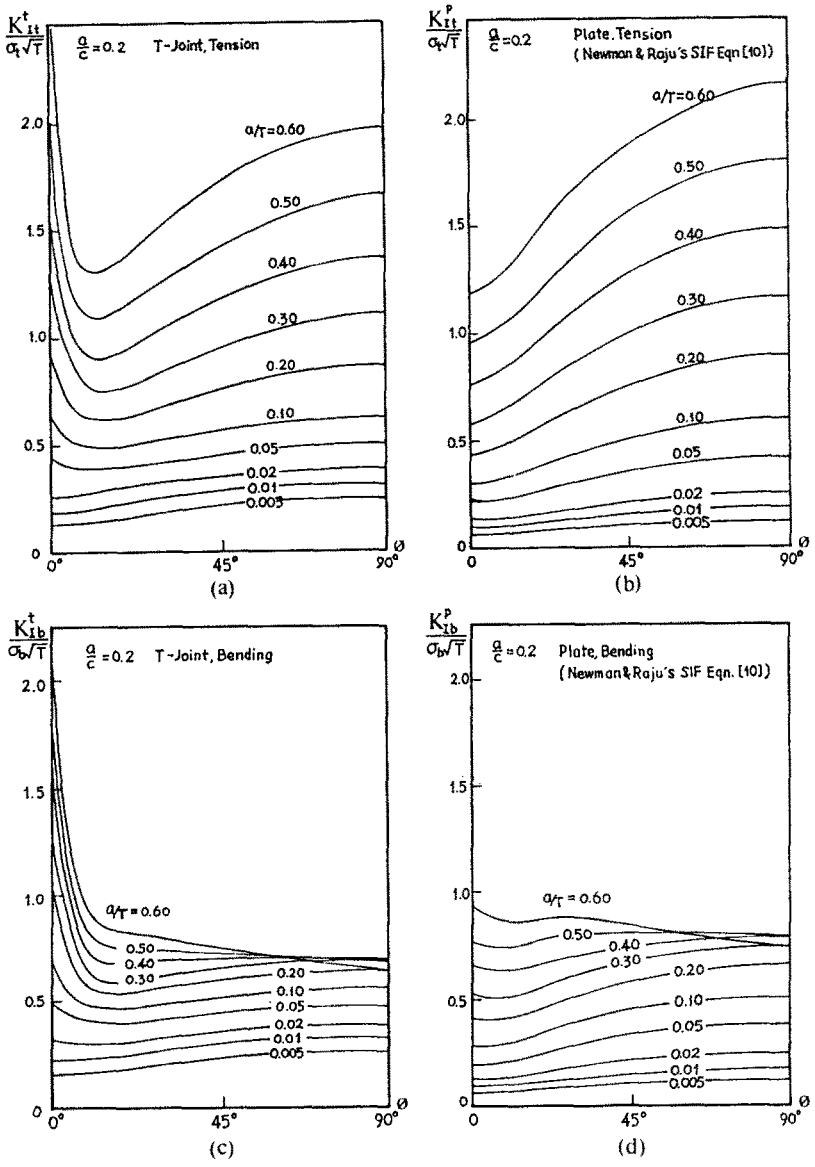

Fig. 12. Comparison of the SIF predictions for the semi-elliptical surface crack shape $a/c = 0.2$, obtained using Newman and Raju's SIF equation [10] with and without the weld correction.

welded T-butt joint models were determined by incorporating the functions in (12)–(14) into Newman and Raju's SIF equations.

The comparison demonstrates the increase in SIF distributions along the shallow surface crack front and along the shallow sections of the deep surface cracks, due to the high M_k values. This implies that the weld-toe surface cracks will grow faster than those in plain plates during the early stage of the fatigue crack growth, and that crack growth along the weld/plate intersection will occur in preference to growth through-thickness. This is generally consistent with experimental crack growth data for welded structures.

6. Conclusions

A detailed 3D LEFM analysis of shallow surface cracks in fillet welded T-butt joints has been carried out using the FE method. The effects of the weld notch and attachment stiffness on the SIF values of weld-toe surface cracks have been studied. Results and conclusions are summarised below.

The FE results indicate that two contradictory effects influence the crack front SIF distribution,

(i) the stress concentration due to the weld-toe notch, and
(ii) the local structural constraint due to the welded attachment.

The effect of the stress concentration increases the SIF values of the shallow crack front and is dependent on the relative depth of each specific crack front point. The effect of local constraint reduces the SIF values for surface cracks with finite lengths, and is dependent on the crack shape aspect ratio for a specific weld geometry. These two effects can be treated separately in the estimation of the SIF.

The weld magnification factors for weld-toe surface cracks have been derived. The present analysis suggests a simple M_k equation in terms of two separate parts, taking account of the two effects respectively. The M_k equation has been derived from detailed 3D FE analysis. It provides a practical approach for engineering analysis.

The SIF distributions predicted for the surface cracks in a weld-toe intersection indicate that shallow fatigue surface cracks in weld notch locations will grow preferentially along the weld toe intersection, i.e. the crack aspect ratio reduces as the weld-toe surface crack grows through the plate thickness. In case of multiple weld-toe cracks, this also implies an enhanced tendency to crack coalescence.

Acknowledgements

The authors wish to thank British Gas plc for permission to publish this paper.

References

1. S.J. Maddox, *International Journal of Fracture* 11 (1975) 221–243.
2. British Standard Published Document PD 6493; Method for the Derivation of Acceptance Levels for Flaw in Fusion Welded Joints, British Standard Institution, UK (1991).
3. I.J. Smith and S.J. Hurworth, The Effect of Geometry Changes upon the Predicted Fatigue Predicted Fatigue Strength of Welded Joints, TWI Report 244/1984, The Welding Institute, Cambridge, UK (1984).
4. X. Niu and G. Glinka, *International Journal of Fracture* 35 (1987) 3–20.
5. S.D. Thurlbeck and F.M. Burdekin, Effects of Geometry and Loading Variables on the Fatigue Design Curve for Tubular Joints, IIW Document XIII-1428-91, International Institution of Welding (1991).
6. I.J. van Straalen, O.D. Dijkstra and H.H. Snijder, in *Proceedings of the International Conference on Weld Failures* (London) (1988) 367–376.
7. O.D. Dijkstra, H.H. Snijder and I.J. van Straalen, in *Proceedings of 8th International Conference on Offshore Mechanics and Arctic Engineering* (Hague) (1989) III.137–143.
8. R. Bell, Stress Intensity Factors for Weld Toe Cracks in Welded T Plate Joints, DSS Contract No. OST84-00125, Faculty of Engineering, Carleton University, Ottawa (1987).

9. B. Fu, J.V. Haswell and P. Bettess, in *Proceedings of the 1st International Conference on Shallow Crack Fracture Mechanics Toughness Tests and Applications*, The Welding Institute (Cambridge) (1992) Paper 22.
10. J.C. Newman and I.S. Raju, *Engineering Fracture Mechanics* 15 (1981) 185–192.
11. H.L.J. Pang, A. Review of Stress Intensity Factors for Semi-Elliptical Surface Cracks in a Plate and Fillet Welded Joint, TWI Report 426/1990, The Welding Institute, Cambridge, UK (1990).
12. J.C. Newman Jr and I.S. Raju, Stress Intensity Factor Equations for Cracks in Three Dimensional Finite Bodies Subjected to Tension and Bending Loads, NASA-TM-85793, NASA Langley Research Center, Virginia, USA (1984).
13. R.S. Barsoum, *International Journal on Numerical Methods for Engineering* 10 (1976) 25–27.
14. *ABAQUS Users Manual* (Version 4.8), Hibbitt, Karlsson and Sorensen Inc, Providence, USA (1989).
15. D.M. Parks, *Computer Methods in Applied Mechanics and Engineering* 12 (1977) 353–364.
16. B. Fu, Variations in Stress Singularity of Surface Cracks and the Effect in Determination of Stress intensity Factor Solutions, ERS R4909, Engineering Research Station, British Gas plc., Newcastle upon Tyne, UK (1992).
17. I.S. Raju and J.C. Newman Jr, *Engineering Fracture Mechanics* 11 (1979) 817–829.
18. *RS/1 Users Guide*, BBN Software Production Corporation, Cambridge, USA (1988).